6ICEGE 6th International Conference on Earthquake Geotechnical Engineering
1-4 November 2015
Christchurch, New Zealand

Characterization of Sequenced Earthquake Motions for Liquefaction Assessment

T. Kobayashi[1], S. Sassa[2], K. Watanabe[3]

ABSTRACT

This study attempts to characterize the generation of excess pore pressure during sequenced earthquake motions. Such sequenced earthquake motions possibly contributed to the devastating liquefaction in coastal areas in the 2011 Tohoku Earthquake. In fact, much evidence of liquefaction was reported at locations where the conventional liquefaction assessment did not predict the risk of liquefaction. To observe excess pore pressure generation during sequenced earthquake motions, a series of shaking table tests were performed with a model ground constructed in a laminar box. The significance of the intensity of earthquake motions and quiet intervals between shocks are examined. Furthermore, the applicability of conventional intensity measures for liquefaction such as shear stress ratio and CAV_5 are studied for sequenced earthquake motions. The analysis shows that, for a certain range of quiet intervals, pore pressure generation during aftershocks can be reasonably explained by conventional intensity measures.

Introduction

The 2011 Tohoku Earthquake in Japan caused massive damage to coastal structures due to ground liquefaction. The earthquake motion is particularly notable for its peak acceleration (2.99 g) and long duration (about 3 min). In conventional risk assessment methods for liquefaction, the intensity of an earthquake motion is characterized by either peak acceleration or shear stress. Such methods, however, do not consider the duration of the earthquake motion. Recently, the Technical Standards and Commentaries for Port and Harbour Facilities in Japan (Ministry of Land, Infrastructure, Transport and Tourism, Japan, 2012) introduced the concept of "effective wave" to account for the duration of the earthquake motion. An effective wave is defined as a wave that exceeds 60% of the peak shear stress during the earthquake motion, and which is thought to contribute to the development of excess pore pressure. Subsequently, the intensity measure of an earthquake motion is modified by the number of effective waves. The number of effective waves becomes as many as 10 in the 2011 Tohoku Earthquake at many locations. Meanwhile, the number is found to be 5 in the 1983 Central Japan Sea Earthquake, which has been used as a basis to establish the present risk assessment criteria for liquefaction in Japan.

Another feature of the Tohoku Earthquake is the frequent aftershocks. Within an hour after the main shock, shocks with magnitude of more than 7 occurred three times with the intervals of 22, 7 and 10 minutes. Such aftershocks may generate additional pore pressure before it fully

[1]Mr. Takaaki Kobayashi, Port and Airport Research Institute, Yokosuka, Japan, kobayashi-t@pari.go.jp
[2]Dr. Shinji Sassa, Port and Airport Research Institute, Yokosuka, Japan, sassa@pari.go.jp
[3]Mr. Keita Watanabe, Port and Airport Research Institute, Yokosuka, Japan, watanabe-k84x3@pari.go.jp

dissipates after the main shock and possibly trigger further liquefaction. In fact, much evidence of liquefaction was reported at locations where the current risk assessment method did not predict the occurrence of liquefaction. This study investigates the mechanism of liquefaction induced by sequenced earthquake motions. A series of shaking table tests were performed with various combinations of a main shock and aftershocks. First, the test procedure is explained. Next, the results of the shaking table tests are described. Finally, the characterization of sequenced earthquake motions is discussed in terms of liquefaction based on the test results.

Materials and Methods

Model Ground

Figure 1 shows a laminar box and a shaking table used in the tests conducted in this study. The laminar box had 29 layers and the inside of the box was covered by a sheet of rubber to avoid interference with shear deformation of the ground during earthquake motions. The design of the model ground is illustrated in Figure 2. The model ground consisted of the base layer made of crushed stone and the top layer made of sand. A sheet of nonwoven textile was placed between the layers to prevent leakage of the sand. The sand used was IIde sand No. 7 whose fundamental mechanical properties are specified in Table 1. After filling the laminar box with water, the sand layer was constructed by repeatedly pouring sand from a certain height to ensure homogeneity of the ground. At different depths in the ground, pore pressure transducers, accelerometers, and total stress cells were installed. The pore pressure transducers and accelerometers were placed in the middle of the ground while the total stress cells were attached to the side wall to measure the lateral stress of the ground.

Figure 1. Laminar box and shaking table

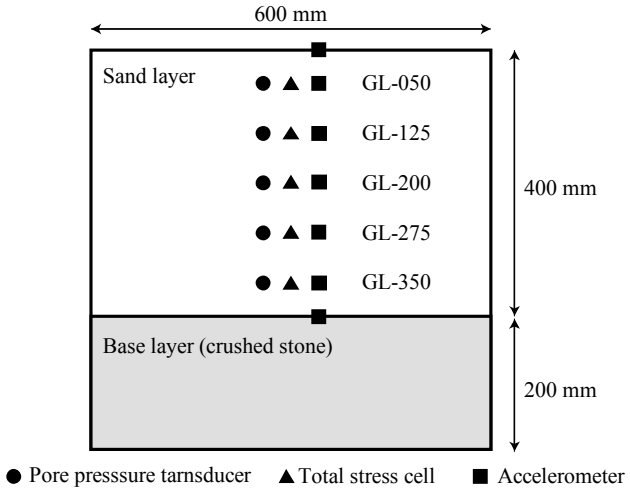

Figure 2. Design of the model ground

Table 1. Mechanical properties of IIde sand No. 7

Particle density	Maximum dry density	Minimum dry density	Median grain size D_{50}
2.652 g/cm^3	1.651 g/cm^3	1.328 g/cm^3	0.18 mm

Input Wave

The input wave was designed by combining the earthquake motions recorded at Hitachinaka during the 2011 Tohoku Earthquake (Figure 3). The soil condition at Hitachinaka can be found at "http://www.eq.pari.go.jp/kyosin/data/pnt/hitachinaka-u.htm". Two equal aftershocks followed the main shock with certain quiet intervals. The peak accelerations were about 600 gal during both shocks and they were reduced proportionally to various levels in the tests. The time scale of the earthquake motions was reduced by a factor of 20 considering rapid dissipation of excess pore pressure in the model ground. Furthermore, the quiet intervals between the shocks were set from 0.3 to 0.7 s. The scaling law regarding the pore pressure dissipation during the quiet intervals is considered as follows. In one-dimensional consolidation theory, a dimensionless time factor T_v is given by

$$T_v = \frac{c_v t}{H^2} \tag{1}$$

where c_v is the coefficient of consolidation, t is time, and H is the distance of seepage. Assuming c_v is constant, fixing T_v in the model ground and the prototype gives the following scaling law regarding the duration of pore pressure dissipation:

$$\frac{(t)_p}{(t)_m} = \frac{(H^2)_p}{(H^2)_m} \tag{2}$$

Note that the subscripts m and p indicate quantities in the model and the prototype, respectively. According to Equation 2, the quiet intervals of 0.3 to 0.7 s correspond to 12.5 to 29.2 min in the prototype ground with a height of 20 m. Therefore, this condition is comparable to what was observed during the 2011 Tohoku Earthquake.

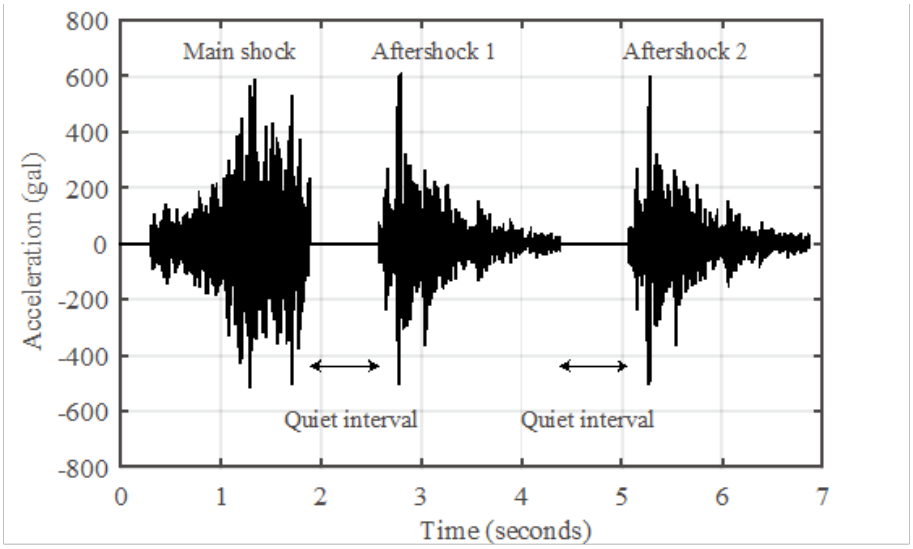

Figure 3. Input wave for shaking table tests

Test Cases

The tests were performed for two different relative densities of the model ground. The first series of the tests, Cases 1 to 5, were performed for a relative density of 45% (Table 2). The intensity of the main shock was adjusted to the level that the excess pore pressure ratio (excess pore pressure normalized by vertical effective stress) increased to about 70% to 80% during the main shock at GL-050 (the shallowest point of observation). The intensity of the main shock was kept constant throughout the test series, while those of the aftershocks were varied. Note that the peak accelerations shown in Tables 2 and 3 are the target values and the observations on the base ground surface in the tests vary by 10% at maximum. Also note that the values of CAV_5 shown here are based on the input waves of which time scale is reduced by a factor of 20. In addition to the intensity of the aftershocks, the quiet intervals between the shocks were varied from 0.7 to 0.3 s to observe their effect on the development of excess pore pressure. In Table 2, shaded cells indicate the test cases in which liquefaction was observed during the test. This will be discussed in detail in the Discussion section. For the second series of tests, i.e., Cases 6 to 9, the same conditions were applied for the model ground with a relative density of 80% (Table 3). The intensities of the input waves were enlarged due to the high density, but the main/aftershock ratios were kept constant between the two series.

Table 2. Test cases for a relative density of 45%; Shaded cells indicate occurrence of liquefaction

Peak acceleration and (CAV_5) during main shock	**Peak acceleration and (CAV_5) during aftershocks**	**Quiet intervals**		
		0.7 s	**0.5 s**	**0.3 s**
182 gal (47.5 cm/s)	**236 gal (49.1 cm/s)**	Case 1		
	182 gal (40.6 cm/s)	Case 2		Case 3
	146 gal (32.1 cm/s)	Case 4		Case 5

Table 3. Test cases for a relative density of 80%; Shaded cells indicate occurrence of liquefaction

Peak acceleration and (CAV_5) during main shock	**Peak acceleration and (CAV_5) during aftershocks**	**Quiet intervals**		
		0.7 s	**0.5 s**	**0.3 s**
332 gal (87.0 cm/s)	**432 gal (90.4 cm/s)**	Case 6		
	332 gal (75.2 cm/s)		Case 7	Case 8
	266 gal (59.9 cm/s)			Case 9

Test Results

The time histories of excess pore pressure during the earthquake motions are shown in Figures 4, 5, and 6. The excess pore pressure ratio was calculated by normalizing the observed excess pressure by the initial vertical effective stress at each location in the model ground. Note that the results are shown only for the shallowest observation point (GL-050) for all test cases where liquefaction was the most significant. First, Figure 4 compares the time histories of excess pore pressure with different aftershock intensities. The main shock intensity and the length of the

following quiet intervals are common in these three cases. Pore pressure generation during the aftershocks was significantly influenced by the intensities of the aftershocks. Secondly, Figure 5 compares the effect of quiet intervals on pore pressure generation in Case 2 (0.7 s) and Case 3 (0.3 s). Due to less pore pressure dissipation during the quiet intervals, liquefaction occurred in Case 3 by the accumulated pore pressure during the two aftershocks. Finally, the effect of the model ground density is illustrated in Figure 6. The intensities of the main shocks were different (182 and 332 gal) but the main/aftershock ratio was essentially the same (about 1: 1) in both cases. The excess pore pressure during the main shocks was comparable but liquefaction occurred in only Case 3. In contrast, excess pore pressure ratio did not exceed 0.7 in Case 8 owing to a low dilatancy potential due to the high density of the ground material.

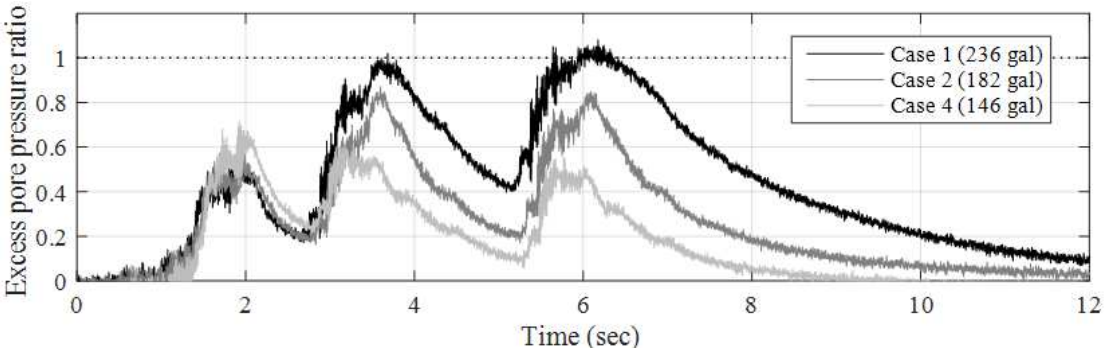

Figure 4. Excess pore pressure ratio for varying intensities of aftershocks (D_r = 45%)

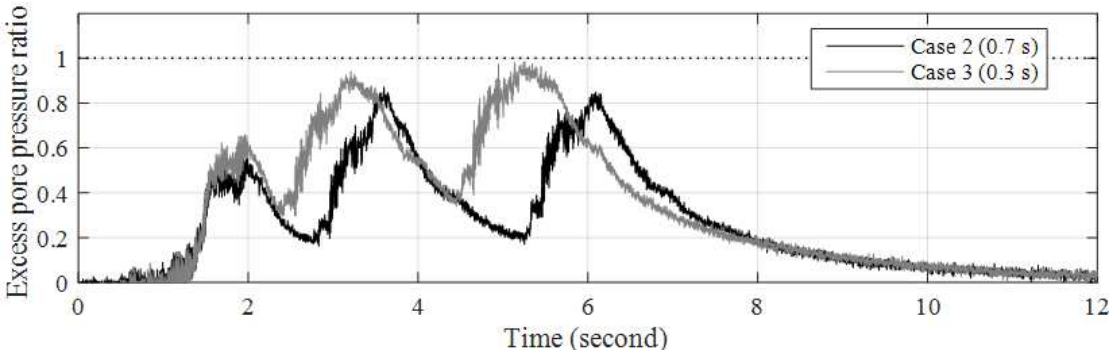

Figure 5. Excess pore pressure ratio for varying quiet intervals between shocks (D_r = 45%)

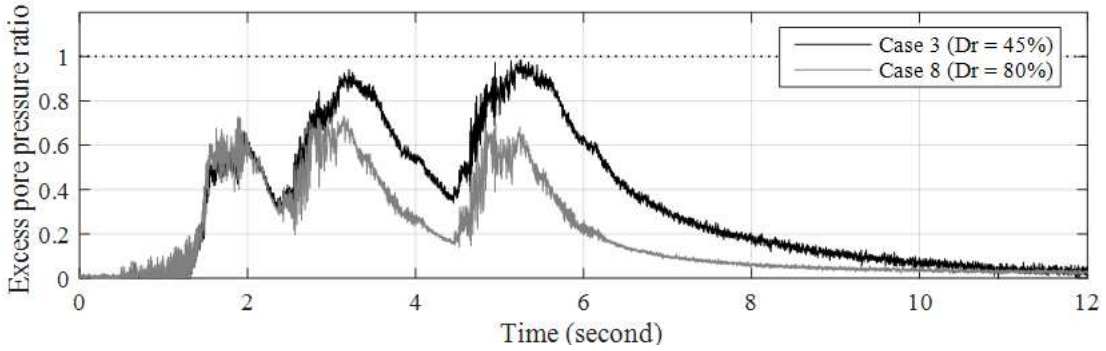

Figure 6. Excess pore pressure ratio for varying relative densities of the model ground

Discussion

In this section, the applicability of conventional intensity measures for liquefaction is examined for the sequenced earthquake motions based on the results of the shaking table tests. We focus only on the generation of excess pore pressure during the first aftershock. It is assumed that the degree of liquefaction during the main shock is comparable within the test series, although some differences exist between the test cases. As a conventional intensity measure, CAV_5 (Kramer et al., 2009) was estimated from the observed acceleration at the surface of the base layer in each of the test cases. CAV_5 is calculated by integrating the acceleration of a ground motion with a threshold of 5 m/s^2 to filter out the low acceleration. According to Kramer et al. (2009), CAV_5 is more closely related to excess pore pressure generation than other intensity measures including Arias intensity (Arias, 1970) and peak acceleration. Figures 7 and 8 show the estimated CAV_5 against the peak excess pore pressure ratio during the first aftershock for relative densities of 45% and 80%, respectively. The shape of the markers indicates the intensity of the aftershock while the color indicates the quiet intervals (See Tables 2 and 3). There seems to be a linear relationship between CAV_5 and the peak excess pore pressure ratio for both relative densities of the model ground. When comparing the tests cases with varying quiet intervals, i.e. Cases 2 and 3 in Figure 7 and Cases 7 and 8 in Figure 8, the effect seems less significant than CAV_5.

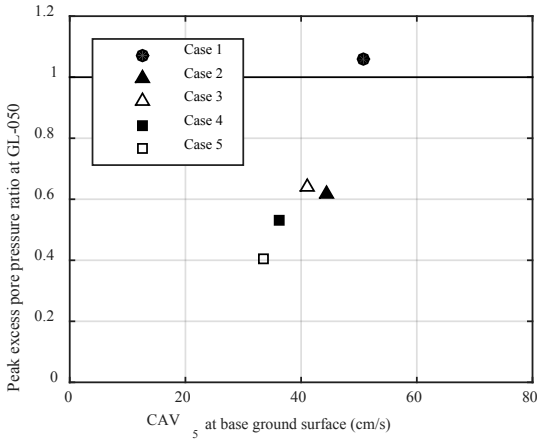

Figure 7. CAV_5 vs. peak excess pore pressure ratio during the first aftershock for D_r = 45%

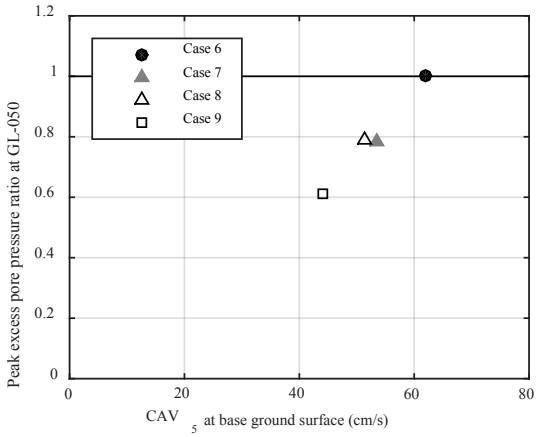

Figure 8. CAV_5 vs. peak excess pore pressure ratio during the first aftershock for D_r = 80%

Next, shear stress ratio (SSR) was evaluated at each depth in the model ground by equivalent linear analysis (SHAKE, Schnabel et al., 1972). Based on the observed acceleration on the base ground surface, response shear stress was calculated by SHAKE. SSR was then found at each depth by normalizing the calculated peak shear stress during the first aftershock by the initial effective vertical stress. Figure 9 and 10 show the observed peak excess pore pressure ratio against estimated SSR at each depth for relative densities of 45% and 80%, respectively. Again, the shape of the markers indicates the intensity of the aftershock while the color indicates the quiet intervals. In Figure 9, the isolated plots in the right hand side correspond to the observations at GL-050 in each test cases where liquefaction is the most significant owing to the low effective stress of the ground. Apart from those points, a linear relationship (the dashed line in Figure 9) is indicated in SSR and the peak excess pore pressure ratio. For a given range of

quite intervals (0.7 to 0.3 s), their effect on pore pressure generation appears less significant than SSR. This linear relationship provides a critical SSR value (0.34) to predict liquefaction during the aftershock in the situation considered in this study. Meanwhile, in Figure 10, the whole plots yield a linear relationship with a lower slope indicating the low liquefaction potential owing to the high density of the model ground. For the relative density of 80%, the critical SSR is found to be 0.57.

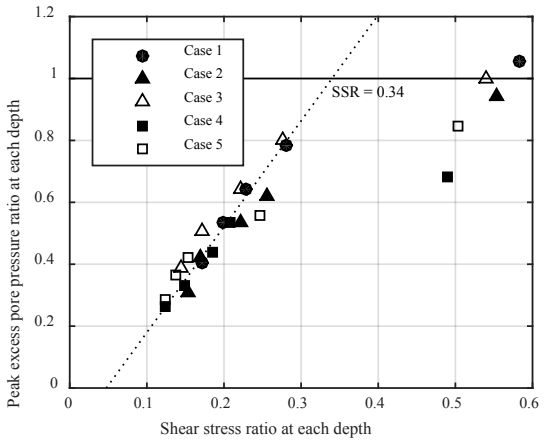

Figure 9. SSR vs. peak excess pore pressure ratio during the first aftershock for D_r = 45%

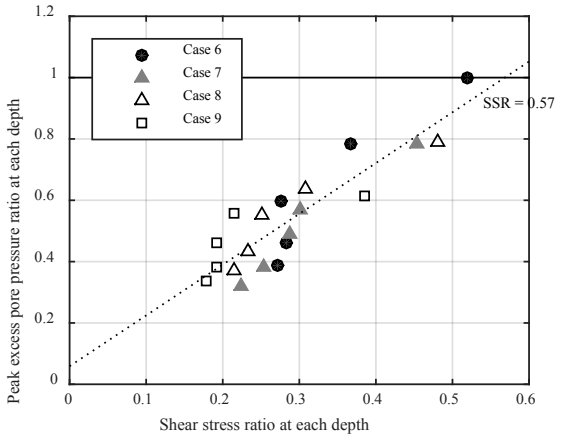

Figure 10. SSR vs. peak excess pore pressure ratio during the first aftershock for D_r = 80%

The test results suggest that, for a certain range of main shock intensity and quiet intervals, the pore pressure generation during an aftershock can be characterized by conventional intensity measures such as CAV_5 and SSR. Further studies are required to examine the limitation of those intensity measures for wider range of main and aftershock intensities, quiet interval and ground material.

Conclusions

The following conclusions are drawn in this study.

1. From the shaking table tests, the effects of the aftershock intensity, the quiet intervals, and the relative density of the model ground on pore pressure generation were observed.
2. CAV_5 and shear stress ratio (SSR) estimated by SHAKE can reasonably explain the pressure generation during an aftershock. For the situation considered in this study, the critical SSR values regarding liquefaction are found be to 0.34 and 0.57 for relative densities of 45% and 80%, respectively.

Further studies are required to clarify the limitation of conventional intensity measures and develop a new liquefaction assessment method for sequenced earthquake motions.

Acknowledgments

The authors gratefully acknowledge the support of the Ports and Harbours Bureau, Ministry of Land, Infrastructure, Transport and Tourism in Japan.

References

Arias, A. *A measure of earthquake intensity. In Seismic design for nuclear power plants (ed. R. J. Hansen)*. Cambridge, MA: MIT Press, 1970; 438– 483.

Kramer S. and Mitchell R. Ground motion intensity measures for liquefaction hazard evaluation. *Earthquake Spectra*, 2006; **22**(2), 413–438.

MLIT: Ministry of Land, Infrastructure, Transport and Tourism, Japan. *Technical Standards and Commentaries for Port and Harbour Facilities in Japan*, 2012.

Schnabel PB, Lysmer J, and Seed HB. *SHAKE: A Computer Program for Earthquake Response Analysis of Horizontally Layered Sites"*. Report No. UCB/EERC-72/12, Earthquake Engineering Research Center, University of California, Berkeley, 1972.